Theoretical Work for the Fast Zero-Power Reactor FR-0

H. Häggblom



AKTIEBOLAGET ATOMENERGI STOCKHOLM, SWEDEN 1965

THEORETICAL WORK FOR FAST ZERO-POWER REACTOR FRO

Hans Häggblom

Abstract

The theoretical part of the fast reactor physics work in Sweden has mainly been connected with the FRO reactor. The report describes the principal features of this reactor, evaluation of cross sections, calculations of critical masses, reactivity of the air gap and of control rods and calculations of neutron generation time and effective beta values. Carlson codes in spherical and in cylindrical geometry are used to evaluate critical masses and fluxes. In cases when reactivity changes are calculated, complementary methods are perturbation theory and variational calculus. The agreement with experiments is in some cases good, especially the determination of critical mass, but in other cases discrepanicies are observed, e.g. the activation of U-238 in the reflector is much larger than the theoretical spectrum predicts.

LIST OF CONTENTS

		Page
1.	Introduction	3
2.	Evaluation of Cross Sections	4
3.	Calculations of critical mass and neutron spectrum	11
4.	The reactivity worth of the air gap	13
5.	Control rod calculations	15
6.	Calculation of neutron generation time and effective beta values	17
7.	General conclusions	19
Ackn	owledgements	20
Refe	rences	21
Table	es	2 5
Figur	res	

1. Introduction

The fast zero-power reactor FR0 which in design features resembles the British Vera reactor became critical in February, 1964. The only available fuel material is 20 % enriched uranium containing 120 kg of U-235, so that the experiments must be done with small cores only. The reactor is built in two halves, each of which consists of a matrix of vertical tubes of stainless steel. These tubes are then loaded with core and reflector materials. During the first year there has been only one type of loading. The core region has been filled with fuel coated with a thin layer of teflon. The reflector region has similarly been filled with copper.

The reactivity of the assembly can be regulated either by varying the gap width between the two halves of the reactor, or by control rods which in their inner position have the same composition as the reactor.

A relatively large part of the theoretical work has consisted of producing cross sections to be used as input data in reactor physics calculations. The principle for this work has been that all data must be founded on differential measurements or, when experimental values are not available, upon calculations using appropriate nuclear models. In some cases we have used the data given in the book of Yiftah, Okrent and Moldauer (ref. 1). In other cases we have tried to obtain data from more recent measurements or by using more advanced theoretical models. Also, by producing group cross sections, we have to some extent considered the effect of selfshielding in the resonance region.

Our most important reactor physics calculations involve determination of critical mass and multigroup spectrum, reactivity worth of control rods and air gap, and determination of neutron lifetime and effective beta values. For the critical mass calculations, DS₄ or TDC programmes have usually been used. Perturbation theory has been used for control rod, air gap, neutron lifetime and effective-beta calculations. For control rod and air gap calculations we have also used the TDC programme and for gap calculations a variational method. These calculations will be described in the following sections.

2. Evaluation of Cross Sections

Two main sets of cross sections have been produced. The first set was finished in 1963 and consists of two subsets which we shall call 1A and 1B. Subset 1A is the principal one and consists of microscopic cross sections in 11 energy groups for the following elements: C, F, Al, Cr, Fe, Ni, Cu, U-235 and U-238 (ref. 2). Some theoretical work has been performed in connection with the evaluation of these data, namely calculation of elastic and inelastic cross sections for U-238 and Cu. Elastic cross sections were calculated using the nuclear optical model where spin-orbit coupling was included in the calculations for copper. The potential functions were of Saxon-Woods' form for the real part and a combination of Saxon-Woods' potential and a Gaussian potential for the imaginary part. Detailed results of these calculations are given in ref. 3 and 4.

For energies which can excite only a few nuclear levels, compound elastic and inelastic cross sections were obtained by Hauser-Feshbach calculations. For copper, the spin-orbit potential was accounted for by a jj-coupling scheme. The differential compound elastic cross sections were then added to the shape elastic cross sections obtained by the optical model. Later measurements by A. B. Smith at A. N. L. (ref. 5 and 6) and by Wiedling et al. at AB Atomenergi (ref. 7 and 8) agree satisfactorily with the theoretical results. Wiedling et al. have extended the optical model calculations and obtained parameter values which still better agree with the experimental results. These data are not yet all published and are not included in our cross section sets.

The Hauser-Feshbach calculations were performed for U-238 below 1.0 MeV and for Cu below 1.75 MeV. Above 1.35 MeV for U-238 and above 1.75 MeV for copper, the inelastic scattering matrix was obtained by means of the statistical model. For U-238, the discrete level formalism is rather arbitrarily extrapolated to the region 1.0 - 1.35 MeV. This was done by introducing two hypothetical levels at 1.0 and 1.2 MeV and by a graphical extrapolation of the calculated partial cross sections so that the total inelastic cross section smoothly connects the theoretical curve up to 1 MeV with the experimental values above 1.35 MeV.

For the other elements, ref. 1 and 9 were the most important sources of information, with the exception that the number of neutrons per fission, v, for U-235 is obtained from more recent measurements. In cases when the starting point was differential data, group cross sections were obtained by averaging with an earlier calculated, approximative spectrum. The first calculations of critical mass and spectrum for FRO were performed using the 11-group cross sections given in ANL-5800 (1958) and the group structure from these calculations was retained in the set 1A. Set 1B, which contains 6 groups, was obtained from set 1A by averaging, using the calculated 11-group spectrum. It is only tabulated in the form of macroscopic cross sections for the FRO assemblies 1 and 2, the compositions of which are given in Table 9.

The cross section set 1 was used until the middle of 1963. After that, new differential data have been evaluated or been moulded into an applicable form. Data tabulated point-by-point exist for the following elements: hydrogen, deuterium, beryllium, boron, carbon, oxygen, fluorine, sodium, aluminium, silicon, calcium, chromium, manganese, iron, nickel, copper, zirkonium, lead, U-235, U-238, Pu-239. The number of energy points was so chosen that the resonances are included whenever data are available and when these resonances do not cause the number of points to exceed about 500. This maximum number is determined by the limited memory space in the machine which has to handle the data and generate group cross sections. For U-238, the resonances are averaged by using the British programme Eric 2 (ref. 10) so that the data here do not contain differential cross sections but group cross sections for very narrow groups and for a specific, very dilute, composition. For U-235, some resonances are considered in a pointwise description but the data extend only down to 100 eV. For the other materials, the data are given from thermal energy to 10 MeV or in some cases to 18 MeV. For each element there is a corresponding tape with punched data.

The differential data have been evaluated in co-operation with the Institution for General Physics at AB Atomenergi. This institution has compiled the data for hydrogen, deuterium, beryllium, boron, carbon, oxygen, sodium, aluminium, silicon, calcium, manganese, zirconium and lead. K. Jirlow has compiled the data for Pu-239 and has evaluated a part of the data for U-238. A reference to the sources from which the data for the rest of the elements were obtained is given below. We use the following symbols for the material constants:

- $\sigma_{T}(E)$ = total cross section at energy E.
- $\sigma_{el}(E)$ = elastic cross section at energy E.
- $\sigma_{C}(E)$ = capture cross section at energy E.
- $\sigma_{in}(E)$ = inelastic cross section at energy E.
- $\sigma_{n,2n}(E)$ = cross section for the (n,2n) reaction at energy E.
- $\theta = \sqrt{\frac{E}{a}}$ = neutron temperature for inelastic scattering at energy E. Only the constant a is given in the data. The same constant is also introduced to describe the secondary neutron energy distribution of the (n, 2n) process.
- $\sigma_{\epsilon_i}(E)$ = cross section for inelastic scattering at energy E associated with excitation of the nuclear energy level ϵ_i .
- v(E) = average number of fission neutrons caused by a fission at energy E.
- $\sigma_f(E)$ = fission cross section at energy E.
- f_k(E) = 1'th Legendre coefficient for the differential elastic cross section, $d\sigma_{el}(\mu)$, at energy E. These coefficients are then defined by the expression

$$2\pi d\sigma_{el}(\mu) = \sigma_{el} \sum_{\ell=0}^{\infty} \frac{2\ell+1}{2} f_{\ell} P_{\ell}(\mu)$$
 (1)

A computer programme, LECOCROSS (ref. 11), was developed to obtain the f₂:s from d $\sigma_{el}(\mu)$ at 11 values of the angular variable μ .

 $\sigma_c(E)$ does not occur on the data tape but is in some cases used to give $\sigma_{el}(E)$ when the other cross sections are known.

The elements for which data are evaluated in connection with work on FR-0 are:

a. Fluorine

The fluorine cross sections are compiled from the following sources:

 $\sigma_{T}(E)$ from ref. 12.

 $d\,\sigma_{\rm el}(E,\mu)$ from ref. 13 and 14.

 $\sigma_e(E)$, $\sigma_{in}(E)$ and $\sigma_{\epsilon_i}(E)$ from ref. 12 and 15.

Above 3.1 MeV, a statistical energy distribution of inelastically scattered neutrons is assumed. The constant a, giving the neutron temperature, is calculated from the approximative formula (ref. 16):

$$a = \frac{B^2}{4} \tag{2}$$

$$B \approx 0.62 \sqrt{A}$$
 (3)

where A = mass number.

b. Chromium

The sources of information are:

 $\sigma_{\rm T}(E)$, $\sigma_{\rm el}(E)$, $\sigma_{\rm in}(E)$ and f_1 from ref. 17. $\sigma_{\rm el}(E)$ from ref. 18.

a from ref. 19.

Discrete inelastic levels are accounted for from 3.31 MeV downwards.

c. Nickel

 $\sigma_{\rm T}({\rm E})$, $\sigma_{\rm el}({\rm E})$, $\sigma_{\rm in}({\rm E})$ and f_1 were obtained from ref. 17, $\sigma_{\rm el}({\rm E})$ from ref. 12 and 20 and a from ref. 19.

Discrete inelastic levels are accounted for from 2.75 MeV downwards.

d. Copper

For $\sigma_{\rm T}(E)$ we use the data in ref. 12. $\sigma_{\rm c}(E)$ is for \geq 10 keV obtained from ref. 12 and 21. In the resolved resonance region, 0.2 < E < 10 keV, $\sigma_{\rm c}(E)$ is calculated in the following way. According to one-level resonance theory we have (ref. 22):

$$\frac{\sigma_{T}}{\sigma_{Y}} = \frac{\Gamma}{\Gamma_{Y}} + 4 k R \left(\frac{E - E_{O}}{\Gamma_{Y}}\right) + \frac{4 \pi R^{2}}{\sigma_{Y}}$$
(4)

where

$$\sigma_{v} = \sigma_{c}$$

 $\Gamma = \Gamma_n + \Gamma_v = \text{total level width.}$

 Γ_{v} = radiative level width.

k = wave number of the neutron.

R = potential scattering radius.

E = resonance energy.

If we write

$$\sigma_{\rm p} = 4\pi R^2 \tag{5}$$

and if the cross sections are given in barns and the energies in eV, we obtain:

$$\sigma_{\gamma} = \frac{\sigma_{T} - \sigma_{p}}{\frac{\Gamma}{\Gamma_{v}} + 2.48 \cdot 10^{-3} \left(\frac{E - E_{o}}{\Gamma_{v}}\right) \sqrt{E \cdot \sigma_{p}}}$$
(6)

We have assumed that Γ_{γ} = 0.5 eV for all resonances. This value is chosen because, according to ref. 23, a somewhat too small resonance integral was obtained when Γ_{γ} was taken as 0.4 eV. Γ_{n} and E_{0} are taken from ref. 24 and σ_{p} is estimated from the same reference so that a resonable σ_{γ} is obtained at energies where the interference term is important.

Below the resonance region we have assumed that the capture cross section obeys the 1/v law. $\sigma_{in}(E)$ is obtained from ref. 4 and 12, $\sigma_{\varepsilon i}(E)$ from ref. 2 and the constant a from ref. 19.

e. U-235

Ref. 17 was used for $\sigma_T(E)$, $\sigma_{el}(E)$, $\sigma_{in}(E)$, $\nu(E)$ and $\sigma_f(E)$. A fictive series of $\sigma_{ei}(E)$ was constructed for $E \leq 2.0$ MeV using the curves in ref. 1. The fictive levels adopted are in MeV: 0.035, 0.075, 0.145, 0.250, 0.325, 0.6, 0.9, 1.25, 1.625 and 1.865. For higher energies where the statistical model is used, a was obtained from ref. 19. The Legendre coefficients were obtained from ref. 13 or were assumed to be the same as for U-238 (see below).

f. U-238

Of the data for U-238, K. Jirlow, (AB Atomenergi, private communication), has evaluated resonance integrals over narrow energy ranges, $\mathbf{v}(E)$, $\sigma_f(E)$ and partly the capture cross sections. The resonance integrals are given as effective cross sections for the mean energy of the respective ranges. Outside of the resonance range the data are obtained in the following way.

- $\sigma_{T}(E)$, $\sigma_{f}(E)$ and $\sigma_{n,2n}(E)$ from ref. 17.
- σ_C(E) from ref. 25 in the region 1-20 keV, otherwise from ref. 12. We have also used data from ref. 25 up to 100 keV, but reactor physics calculations will then give worse agreement with experiments.
- $\sigma_{in}(E)$ for E > 1.35 MeV from ref. 17. For $E \le 1.35$ MeV from ref. 2 and 26.
- $\sigma_{\epsilon_i}(E)$ and $f_L(E)$ from ref. 2 and 26.

The statistical model for inelastic scattering is applied above 1.35 MeV. The constant a is obtained from ref. 19.

v(E) is described by a linear function: v = 2.42 + 0.14 E where E is given in MeV. The constants are approximately the same as in ref. 27.

From the differential data we obtain group cross sections in the following way. The neutron spectrum for a given material composition and for a given geometrical buckling is calculated by a computer code, NESPECO, which solves the transport equation in B₁ approximation using the differential material constants as input data. The group cross sections are then obtained by averaging over this spectrum or over an optional input spectrum. The programme can also calculate better guesses for the buckling and for the spectrum in an iterative way if the medium is multiplicative. For a non-multiplicative medium one can obtain an approximative space-dependence of the flux by summation of solutions for a large number of bucklings. The code is described in ref. 28.

By cross section set 2 we mean a series of group cross sections calculated by using the NESPECO programme. The number of groups is 14, 11 and 6.

Microscopic and macroscopic group cross sections have been calculated, the former ones for most of the elements for which punched data are available, using the FR-0 core 1 spectrum, and in some cases also using the reflector spectrum. Work is in progress to improve these sets by using shielded microscopic fuel cross sections which are calculated for the right composition and geometry.

Tables 1 - 8 show 14-group cross sections from set 2 for chromium, iron, copper, U-235 and U-238. In the tables the 14 energy groups are grouped together into cross section groups. The order of these is:

- 1. Vo if not equal to zero
- 2. Transport cross section, σ tr
- 3. Non-elastic cross section, $\sigma_{ne} = \sigma_{tr} \sigma_{el}$
- 4. Total cross section, σ_{T}
- 5. Elastic cross section, $\sigma_{el} = \sigma_{g,g}$
- 6. Removal cross sections from group g to group g, $\sigma_{g,g}$

The group cross sections are defined in ref. 28. Two types of spectra have been used in the averaging for the last three materials. The difference between the corresponding cross sections is largest for copper because the reflector consists to 88 % of this material and because the copper data include all resolved resonances.

3. Calculations of critical mass and neutron spectrum

The criticality calculations were performed using the Carlsson codes DSN and TDC in S₄ approximation. Diffusion theory gives results which deviates from the S₄ approximation by the order of 15 % in critical mass. Two different core compositions and two reflector compositions have been considered in the calculations for FR0 and, in addition, calculations on four assemblies of ZPR III have been performed to obtain additional possibilities of comparing the results with experiments. The compositions of the cores and of the reflectors are given in volume percent in table 9. Assembly 1 consists of core 1 and reflector R1, assembly 2 of core 2 and reflector R1.

Table 10 shows the lower energy boundary and the fraction of fissions in each energy group for different cross section sets. When 11 and 6 groups are used in cross section set 2, the lowest energy boundary is the same as for group 14 in the same set, namely 120 eV.

Table 11 shows the calculated critical radii and masses for different assemblies. Most of the calculations were performed in spherical geometry using the DSN-code. The experimental assembly was first constructed as a cylinder with a diameter-to-height ratio near to 1. The theoretical form factor was obtained from 6-group calculations using the same cross section sets in spherical and in cylindrical geometry. Using set 1 we obtain the form factor $\alpha = 0.950$, using set 2 we obtain $\alpha = 0.934$. The experimental value is 0.961. The TDC value of 71.0 kg for the critical mass was obtained for 40 radial and axial divisions and for a convergence "radius" of 10^{-2} . For 20 radial and axial divisions and a convergence radius of 10^{-3} we obtained a critical mass of 71.3 kg.

The experimental critical mass for assembly 1 with 35 cm reflector is 71.9 kg and is 70.1 kg for assembly 2. An increase in the reflector thickness from 30 to 35 cm does not give any decrease in the calculated critical mass. From table 11 we then observe that cross section set 1 gives better agreement with experiments than set 2 when we only consider FR 0 assemblies 1 and 2. This is, however, not the case when we consider also the calculations for ZPR III. All the calculations using set 1 give too large critical masses, in contrast to set 2 and to, e.g., the Yiftah-Okrent-Moldauer cross sections. The largest positive error is for ZPR III/16 for which the calculated mass is 7.4 % too high. Now assembly 16 is approximately obtained from assembly 12 by substituting a part of the carbon content by U-238. This fact indicates that the high critical mass is due to the U-238 cross sections. For this element the sets 1 and 2 differ mainly in σ_{in} and σ_{c} . The influence of σ_{in} is studied by using a cross section set consisting of the first four groups of set 1 and of the last ten groups of set 2. The critical radius was then only slightly higher than when using a pure cross section set 2. From this we draw the conclusion that the difference in capture cross sections which, in the energy range 0.11 - 1.35 MeV, is about 3 % is the main source of the difference in critical mass. The capture cross sections are also higher in the data of ref. 17. The error in the calculation for ZPR III/16 is one reason why we believe that these data are not better than the BNL-325 values which we have used. Experimental data obtained by Smith (ref. 37) also confirm the BNL-325 data. We have also used the data of ref. 25 up to 100 keV instead of to 20 keV but then the critical mass of FR 0 assembly 2 decreased by 3 %. - One possible cause of the too low critical mass obtained with set 2 lies in the fission cross section of U-235 which, according to recent British measurements (ref. 25), is about 5 % lower than the BNL-325 values.

It is interesting to note the change in critical mass when we go from a larger number of groups to a smaller. The general trend seems then to be that the mass decreases. The difference is due, of course to a wrong choice of weighting function by averaging. To obtain as small an error as possible in the eigenvalue, one should use as weighting function the product of the flux and the adjoint flux (ref. 38). The least satisfactory result is

obtained using cross section set 1, where a very rough approximation of the neutron spectrum is used to reduce the 11-group constants to 6-group constants. In cross section set 2 the same fine-structure spectrum is used to calculate both the 14-group and the 6-group constants. The difference in critical masses is then only about 1 %.

Fig. 1 shows the flux per unit lethargy for assembly 2 in the centre of the core. Fig. 2 shows the corresponding flux in the reflector at 3 cm from the core boundary. Fig. 3 shows the fluxes in the energy groups 1, 5, 9 and 13 as functions of the radius. Comparisons with experiments indicate that the core spectrum is calculated with sufficient accuracy, but the reflector flux appears to be much softer than the calculations show. We have as yet no explanation of this fact. A complete description of the experiments and comparisons with theory will be given by other authors in ref. 39.

Calculations have also been made of the critical mass for different reflector thicknesses of assembly 2. Experiments with different reflector thicknesses have only been performed in cylindrical geometry and keeping the bottom and top reflector thicknesses constant. Corresponding critical mass calculations will be reported in ref. 39.

A limited amount of natural uranium is available for eventual use as reflector material. Some calculations have been performed to find out whether we can obtain a critical system with this reflector.

4. The reactivity worth of the air gap

Air gap calculations are connected with the solution of the transport equation in two dimensions. This was first done by means of perturbation theory and variational calculus in one energy group (ref. 29). The perturbation method developed by Friedman (unpublished paper) was extended to larger air gaps by the variational method. Only a bare reactor is considered in these calculations. The results are compared with those based on diffusion theory and the "direct leakage calculus"

developed by Chernick and Kaplan (ref. 30). It is not possible to make quantitative comparisons with the experiments because of the influence of the reflector in FRO. For small air gaps, diffusion theory gives half as large a reactivity value as the transport theoretical perturbation method. The experimental values will here approximately follow the curve given by diffusion theory. But the reflector will probably decrease the reactivity worth of the gap, and this may be the explanation of why transport theory seems to fail.

The reactivity worth of the air gap has also been calculated using the TDC code and 6 energy groups (ref. 31). Here the calculations were made for the actual reactor. The results of all four types of calculations are given in fig. 4. The TDC calculations give a very low initial reactivity. The experimental values are preliminary and are therefore not given in the figure, but the whole curve is below these values. The reason for this has not yet been explained.

For large air gaps the reactivity was determined experimentally from the counting rate of neutrons round the periphery of the reactor. If this rate is n, the multiplication factor, k, is obtained from the formula

$$n = \frac{n_0}{1-k} \tag{7}$$

n_o is related to the multiplication factor for small air gaps. A corresponding theoretical determination of the reactivity was made by calculating the flux caused by a fixed source for different air gaps (ref. 32).

For a large air gap the reactivity change obtained in these calculations was larger than any other theoretical value. This indicates that the reactivity defined by Eq. 7 is not necessarily the same as that obtained from the eigenvalue of the static transport equation.

5. Control rod calculations

The reactivity worth of the control rods was calculated by two different methods, namely perturbation theory and 6-group TDC calculations. The perturbation theory is based on the transport equation and makes use of a flux obtained from a 1-group P_3 -calculation (ref. 33 and 34). In P_N approximation with an arbitrary number of groups, the perturbation expression for reactivity is

$$\frac{\Delta v}{v} = A^{-1} \left\{ \sum_{g'} \sum_{g'} \int \left[\chi_g \Delta (v \Sigma_f)_{g'} + \Delta \Sigma_{g'g} (1 - \delta_{g'g}) \right] \psi_{g,o}^{+}(\underline{r}) \psi_{g,o}(\underline{r}) dV \right\}$$

$$-\sum_{g} \sum_{n=0}^{N} (-1)^{n} (2n+1) \int \Delta \left(\sum_{g} - \sum_{gg} f_{n,g} \right) \psi_{g,n}^{\dagger} (\underline{r}) \psi_{g,n} (\underline{r}) dV$$
 (8)

where the operator Δ causes a small change in the operand,

v = average number of fission neutrons,

 X_{α} = fraction of fissions in group g,

 $\Sigma_{f,g}$ = fission cross section in group g;

 $\Sigma_{g'g}$ = removal cross section from group g' to group g,

 Σ_{σ} = total cross section in group g,

f = n'th Legendre coefficient of the elastic cross section in group g,

 $\psi_{g,n}^{+}(\underline{r}) = n$ th Legendre coefficient of the adjoint flux in group g.

 $\psi_{g,n}(r) = n$ th Legendre coefficient of the neutron flux in group g,

and

$$A = \sum_{g} \sum_{g'} \int \chi_{g} (\nu \Sigma_{f})_{g'} \psi_{g,o}^{\dagger}(\underline{r}) \psi_{g',o}(\underline{r}) dV$$
 (9)

The advantage of P_N approximation instead of diffusion theory is, above all, that all coefficients are finite also for channels. The gradient

term in diffusion theory is replaced by a sum containing higher Legendre coefficients of the flux.

In the TDC calculations (ref. 31) cross section set 1 was used in connection with a geometric division number of 25 in both directions. These calculations are the most complete ones, but the agreement with experiments is not satisfactory. For cross section set 2 we have used 40 radial and axial divisions but only one reactivity change was calculated, namely the change when the rod is pulled down 20 cm from its inner position. The corresponding reactivity change was in this case in good agreement with the experiments. For all TDC calculations the rod must, of course, be placed in the centre of the reactor.

Fig. 5 shows the results for a central control rod obtained from perturbation calculations and from TDC calculations. The crosses represent experimental values for a control rod at the radial distance 10 cm from the axis. These values were multiplied by the factor 1.54, which is the relative reactivity coefficient for copper in the centre and at the actual radial point. The calculation using cross section set 2 indicates that good results can be obtained with the TDC code if the number of geometrical divisions is sufficient. But to arrive at more definite conclusions, more points have to be calculated and a more systematic investigation must be made of the effect of the geometrical divisions and of the number of necessary iterations.

The total reactivity of the rod was calculated with good accuracy by perturbation theory but this may be fortuitous, because the one-group cross sections give an error in the critical mass of 31 %. The curve in fig. 5 holds for this erroneous critical mass. There are probably two main reasons for the knee in the curve, namely:

1) The theory does not account for the flux deformation. The sharp reactivity decrease up to d = 30 cm is theoretically caused by inserting reflector material in the core as an absorber. The corresponding decrease in the flux will decrease the negative reactivity effect.

2) The flux variation over the cross section of the rod is not considered in the calculations. Thus, at the centre of the reactor, there is no contribution from n-values higher than zero to $\Delta v/v$ (see Eq. 8), and the derivative of $(-\rho)$ is negative in this point which corresponds to d=45 cm in fig. 5. But for non-zero rod cross sections the average over the cross section of higher Legendre moments of the flux is not zero and thus the derivative of $(-\rho)$ is at least less negative than calculated, perhaps always positive for the cross sections in question.

The next step in the perturbation calculations will therefore be to take account of the variation of the flux over the rod cross section and to make calculations in more than one energy group. In preparation for this a new P3 programme in spherical geometry was developed (ref. 35). This programme eliminates all explicit boundary conditions by using an integral transform. The P_N equations are thus transformed to a system of integral equations which are solved iteratively. It turns out that the flux will be calculated with the same order of accuracy as by S₄ calculations within the reactor, also at inner boundaries. This is probably because we do not need to introduce any "artificial" boundary conditions as in diffusion theory and in conventional \boldsymbol{P}_{N} calculations. At the outer boundary, however, the flux is not equally well described because of the discontinuous angular dependence at this point. But for a reflected system this behaviour does not have much effect upon the reactivity and this quantity is then calculated with the same order of accuracy as in S_4 calculations. The computation time is, however, comparatively long but we expect that it can be significantly shortened by further developments.

6. Calculation of neutron generation time and effective beta values

Two different methods were used to calculate the reactor constants which determine the kinetic behaviour (ref. 36).

The first method involved the use of DS_4 calculations to obtain some reactivity values needed. The effective beta values were calculated

by introducing an equivalent removal cross section of the following form:

$$\Sigma_{d,g\rightarrow g} = \sum_{i,j} f_{i,g}, \beta_{i}^{(j)} (v \Sigma_{f,j})_{g}$$
(10)

Eq. (10) describes a removal of neutrons from group g, where a fission occurs in material j, to group g', where some delayed neutrons appear. These belong to the delayed neutron group i; f, is the relative number of neutrons coming into energy group g' and $\beta_i^{(j)}$ is the delayed neutron fraction in the i'th group caused by fission in material j.

First we calculate the critical radius obtained when the delayed neutrons are introduced in the transport equation by the aid of Eq. (10). Then we add to $\Sigma_{d,g\to g}$, the contribution of a particular $\beta_{i,j}$ times a suitable factor n and calculate the corresponding reactivity change, ρ_{\bullet} . The effective beta value is then

$$\beta_{i, \text{ eff}}^{(j)} = \frac{\rho}{n} \tag{11}$$

The results of these calculations are given in table 12. In this case, as for all calculations in this section, cross section set 1 was used.

The neutron generation time is calculated from the reactivity change, $\rho_{\mathcal{T}}$, caused by introducing a term in the transport equation corresponding to the exponential decay constant, \mathcal{T}_{\bullet} The generation time, Λ_{\bullet} is then:

$$\Lambda = \tau \, \rho_{\tau} \tag{12}$$

Table 13 shows the results for $\tau = 10^{-5}$ and 5×10^{-7} seconds.

The second method we have used for calculating $\beta_{i, \text{ eff}}^{(j)}$ and Λ is that of perturbation theory. The neutron flux and the adjoint flux were then computed using a programme for diffusion theory. Several different kinds of perturbations were used to investigate the effect of the deformed flux. The

largest reactivity change was 0.013 and the difference between the results for the different cores is very small. A representative number for the neutron generation time is:

$$\Lambda = 5.4 \times 10^{-8} \text{ s}$$

Corresponding representative values for $\beta_{i,\,\,\mathrm{eff}}^{(j)}$ are given in table 14. From tables 12 - 14 we conclude that calculation of effective beta values by the first method gives results which differ appreciably from those obtained by the second method. For U-238 the first method gives the highest values, while for U-235 the difference between the results has the opposite sign. The reason for the large discrepancies may be that the first method uses S_4 calculations and the second diffusion calculations, or that large errors are introduced in the first method because the reactivity is the difference between two nearly equal numbers.

The generation times calculated by the different methods are more equal for small reactivity changes. The value calculated by the DS₄ method for 8.66 % reactivity increase cannot be compared with the perturbation calculations. But comparing Λ for small ρ -values with the corresponding experimental results, the calculated value is too small, indicating that the flux is too hard.

7. General conclusions

As could be expected from results at other laboratories, the critical mass of such a small system as FR0 can be calculated with acceptable accuracy using several different cross section sets. But we thought it worth while to develop a cross section set of our own because the inaccuracies in the data are then better known. The changes made by us in the differential data to obtain better agreement with experiments concerning integral data are then limited to ranges where such changes are plausible. For instance, we do not believe in the motivation for significant changes in $\sigma_{\rm in}$ below 1 MeV or $\sigma_{\rm c}$ above 30 keV for U-238.

For copper no complete data were available. Therefore the copper cross sections are the most uncertain ones, and this may be the explanation why the calculation of an "average flux" in the reflector does not agree with experiments. This average flux is defined by activation measurements using foils of U-238. The weighting function has then a high value in the low energy region and this is why we conclude that the flux in the reflector is softer than calculated. The too low neutron generation time also tells us that the calculated flux is too hard but in this case we do not know where in the reactor the error is localized. Some, but not all, experiments, however, indicate that the spectrum is calculated with much better accuracy in the core. And it remains still to find out whether copper cross sections can be evaluated which give both the right critical mass and the right spectrum. For instance, an improvement in the values of σ_c in the region 0.1 - 10 keV caused an appreciable increase in the flux in this region, but at the same time the critical mass decreased by 3 % and the influence on the average flux was very small.

The accuracies of the calculational methods are also to some extent unknown. The error in the cylindrical form factor is an indication of an error either in the DS₄ or the TDC calculations. It would be of value to compute the critical masses by other corresponding codes for comparison.

TDC calculations are generally very time-consuming and should therefore be avoided when many calculations are needed for solving one problem, e.g. if we want reactivity values as a function of a continuously varying parameter. In many such cases it is possible to use perturbation theory.

Acknowledgements

We should like to thank mr. S. Pålsson who has performed the computations on the IBM-7090 machine and the Research Institute for National Defence, Stockholm, for permission to use their computer.

References

- 1. YIFTAH S, OKRENT D and MOLDAUER PA Fast Reactor Cross Sections Oxford, Pergamon Press, 1960
- 2. HÄGGBLOM H
 Reactivity Calculations for FR-0 Using Group Cross Section
 Set MIC 0163, 1963
 AB Atomenergi internal report (RFR-227)
- 3. HÄGGBLOM H
 Fast Elastic and Inelastic Cross Sections for U-238, 1962
 AB Atomenergi internal report (RFR-191)
- 4. HÄGGBLOM H
 Scattering Cross Sections for Copper, 1963
 AB Atomenergi internal report (RFR-223)
- 5. SMITH A B
 Scattering of Fast Neutrons from Natural Uranium
 Nuclear Physics, 47, 1963, 633-651
- 6. SMITH A B (compilator)
 Reports to the AEC Nuclear Cross Sections Advisory Group
 Meeting 1964
 (WASH-1046) p. 4 and 7
- 7. ANTOLKOVIC B, HOLMQVIST B and WIEDLING T Fast Neutron Elastic Scattering Cross sections of Fe, Co and Cu, 1964
 AB Atomenergi internal report (RFX-360)
- 8. HOLMQVIST B and WIEDLING T Inelastic Neutron Scattering Cross Sections of Cu and Cu in the Energy Region 0.7 to 1.4 MeV, 1964 (AE-150)
- 9. DAVEY W G
 Calculations for 22 ZPR-III Fast Reactor Assemblies Using
 ANL Cross-Section Set 635, 1962
 (ANL-6570)
- 10. SUMNER H M
 Eric 2, A Fortran Program to Calculate Resonance Integrals and from them Effective Capture and Fission Cross-Sections, 1964 (AEEW-R 323)
- 11. HÄGGBLOM H
 Fast Elastic and Inelastic Cross Sections for U-238, 1962
 AB Atomenergi internal report (RFR-191)
- 12. HUGHES D J and SCHWARTZ R B Neutron Cross Sections, 1958 (BNL 325, 2. Ed.)

- 13. HUGHES D J and CARTER R S
 Neutron Cross Sections, Angular Distributions, 1956
 (BNL 400)
- 14. BEYSTER JR
 Predictions of Fast Neutron Scattering Data with A Diffuse Surface
 Potential Well, 1956
 (LA-2099)
- DAY R B and WALT M
 Gamma Rays from Neutron Inelastic Scattering in B 10, F 19 and Fe 56
 Phys. Rev., 117 (1960), 1330
- 16. WEINBERG A M and WIGNER E P
 The Physical Theory of Neutron Chain Reactors
 Chicago Press, 1958
- 17. SCHMIDT J J
 Neutron Cross Sections for Fast Reactor Materials, 1962
 (KFK 120)
- 18. van PATTER D M et al.
 Gamma Rays from Inelastic Neutron Scattering in Chromium
 Phys. Rev., 128, (1962) 1246
- 19. BARR D W Interpretation of Experimental (n, 2n) Excitation Functions Phys. Rev., 123, (1961) 859
- 20. JACKIW R W et al.

 Calculation of Inelastic Neutron Cross Sections for Even-Even
 Nuclei, A = 46 100, 1961

 (TID 14206)
- 21. DIVEN B C et al.
 Radiative Capture Cross Sections for Fast Neutrons
 Phys. Rev., 120, (1960) 556
- 22. DRESNER L
 Resonance Absorption in Nuclear Reactors
 Oxf. Pergamon Press, 1960
- 23. TRALLI N
 Some Neutron Cross Sections for Multigroup Calculations, 1958
 (APEX-467)
- 24. HUGHES D J et al.

 Neutron Cross Sections, Suppl. No 1, 1960
 (BNL 325, 2. Ed.)
- 25. RAE E R et al.
 Neutron Interactions with Reactor Materials
 Third United Nations International Conference on the Peaceful Uses of Atomic Energy, Geneva 1964, P/167

- 26. SMITH A B
 Scattering of Fast Neutrons from Natural Uranium Nuclear Physics, 47, (1963), 633
- 27. Reactor Physics Constants, 1963, (ANL-5800, 2. Ed.)
- 28. HÄGGBLOM H and NYMAN K
 Nespeco, ett program för beräkning av neutronspectrum
 och grupptvärsnitt i ett ändligt, homogent medium, 1964
 AB Atomenergi internal report (RFN-173) (In Swedish)
- 29. HÄGGBLOM H

 The Reactivity of a Central Air Gap in a Bare Reactor, 1961

 AB Atomenergi internal report (RFR-138)
- 30. CHERNICK J and KAPLAN I
 The Nuclear Reactor with a Transverse Air Gap
 J. Nucl. En., 2, 1955, 41-5!
- 31. HÄGGBLOM H
 Kriticitets-, styrstavs- och luftgapsberäkningar för FR-0
 med den två-dimensionella koden TDC, 1964
 AB Atomenergi internal report (TPM-RFR-308) (In Swedish)
- 32. HÄGGBLOM H
 The effect of the Air Gap on the Flux in FR-0/A in the Presence of an Outer Circular Source, 1965
 AB Atomenergi internal report (TPM-RFR-435)
- 33. HÄGGBLOM H
 Control Rod Calculations for FR-0 using 1-group Transport
 Theory, 1961
 AB Atomenergi internal report (RFR-110)
- 34. HÄGGBLOM H
 Styrstavsberäkningar för FR-0 med kopparreflektor, 1963
 AB Atomenergi internal report (TPM-RFR-258) (In Swedish)
- 35. HÄGGBLOM H
 A P_N Approximation Using Integral Transforms, 1965
 AB Atomenergi internal report (RFR-418)
- 36. HÄGGBLOM H
 Calculation of Effective Beta-values for the Swedish Fast
 Zero-power Reactor, FR-0, 1963
 AB Atomenergi internal report (RFR-253)
- 37. SMITH A B
 Recent Changes in Heavy Element Cross Sections, 1963
 (ANL-6792) p. 29

- 38. MARCHUK G I
 Numerical Methods for Nuclear Reactor Calculations
 Transl. fr. Russian. New York, Consultants Bureau, Inc., 1959
- 39. ANDERSSON T L, HELLSTRAND E, LONDEN S-O and TIRÉN L I Experimental Studies on Assemblies 1 and 2 of the Fast Reactor FR0. Part 1. 1965 (AE-195)

Table 1
Chromium 14-group cross sections averaged over FRQ; core 1 spectrum

2 • 17 5 1 4 2 • 669 78 16 • 56 169	2 • 46966 5 • 86729 15 • 52600	2 • 442 65 6 • 11002 4 • 61562	2.38969 5.41868 4.25956	3 • I 4 4 2 3 3 • 7 0 7 4 7	^σ tr
0.91391 0.23565 0.92837	0.63099 0.31610 0.09611	0 • 3 428 4 0 • 1977 5 0 • 0 40 55	0.24505	0.13159 0.10807	σne
3 • 4 5 6 5 1 2 • 9 5 4 4 3 1 0 • 7 7 2 6 3	3.11406 6.21471 15.72616	2 • 9 I 43 I 6 • 402 I 6 4 • 67 49 7	2 •8 4039 5 • 59800 4 • 3 138 4	3 • 59 • 42 3 • 769 72	$\sigma_{ extbf{T}}$
1.26123 2.43414 15.61332	1.83867 5.53119 15.42989	2 •09981 5•91227 4•57507	2.14464 5.34558 4.18411	3.01265 3.59940	σ _{el}
o •37933			σ _{1,2} 2		
0 +3 4308	0 42 50 17		⁰ 1,3	°2,3	
0 •09 774	0.16075	0.27823	etc.		
0 •0 409 5	0 •09939	0.01796	0.21463		
0 60 18 68	0 • 0 41 56	0.01570	0.00092	0.12557	
0 •00 98 I 0 •2 2 9 4 4	0.01860	0 •00889	0.00085)	

Continued

						* *		
						E01 E0	400	0
						0 0	0 0	0
			0	80000+0		£4 0000 0	*000Ts	, 0
				•	•	98	280•0	0
						0 0	0 0	0
			٥	91000*0	22100.0	99100°0	oS 000°	• •
							07756	
						0 0	0 0	ప
			٥	1700000	1 2000.0	0200000	\$9 000 °	, 0
						9 = 660 0 0		
			0	1100000	\$\$000 * \$	6100000	<u> </u>	, o
					-	. \$\$\$90*0	. 0 0	o
			٥	0\$ 0000 0	0 •00 103	0110000		
						\$ 006I	*00	0
			o	6800000	⊅ L ₱ 00 • 0	1490000		
	- S	- 4				2.1	608°0	٥
1 ə	Q5*8	8°T ₀ .	O	1700000	0 8 8 0 0 0	0 *000 13		

Table 2

Iron 14-group cross sections

averaged over FRO 1 core 1 spectrum

2•22622 2•72668 8•94945	2.28154 3.29790 5.82603	1.92409 4.11350 7.85197	2+31733 8+22193 10-88066	3•12069 2•77880	σ _{tr}
0+97191 0+11772 0+24184	0.86549 0.15910 0.10609	0.51724 0.16315 0.06163	0.18984 0.07640 0.12462	0.17238 0.07486	o ne
5+38662 2+93505 9+05465	2*88334 3*46626 5*89513	2 • 39 28 1 4 • 259 43 7 • 9 4608	2.80693 8.40827 11.01060	3.51699 2.81462	$\sigma_{ ext{T}}$
1-25432 2-60895 8-70761	1 • 41 60 6 3 • 1 388 0 5 • 7 1 9 9 4	1•40685 3•95035 7•79034	2.12749 8.14553 10.75604	2*94831 2*70395	^o el
0.61523			°1,2		
0.15655	0•52594	·	°1,3	^σ 2,3	
0+08938	0.30223	0.19232	etc.		
0.04708	0.02793	0.11095	0.18400		
0+02373	0 0.0932	8 0 0.1	6638	•	
0.01110 0.11112	0.00001	0.06346	o o		

Continued

0.00592 0.00003 0.03563 0 0 0_{1,8} o_{2,8} etc.

0.00505 0.00003 0.02707 0 0
0.00147 0.00001 0.00876 0 0
0.0032 0.00000 0.00135 0 0
0.00374 0.00001 0.00015 0 0
0.00374 0.00001 0.00015 0 0
0.023182

0.00400 0.00002 0 0 0 0 0 0 0 0 0.09476

0.00094 0.00000 0 0 0 0 0 0 0 0 0 0 0.04769

Table 3
Copper 14-group cross sections
averaged over FRO core 1 spectrum

2 • 421 82 4 • 603 16 7 • 99295	2 • 5 9 7 6 4 4 • 9 0 7 7 8 8 • 1 6 3 9 4	3.11640 5.34850 11.04231	3.62942 6.67159 6.68465	4.29019 9.82422	σ _{tr}
1.32471 0.25016 0.34074	0.81056 0.24276 0.34977	0.50344 0.31219 0.12853	0.29395 0.40466 0.11828	0.28549 0.19069	σne
3.45820 4.83700 8.07401	3 • 14771 5 • 05 136 8 • 24672	3 • 5 1 6 5 4 5 • 4 1 3 7 9 1 1 • 1 5 7 9 2	4.04512 6.73808 6.75421	4.66254 9.92627	$\sigma_{ extbf{T}}$
1.09711 4.35300 7.65221	1.78709 4.66502 7.81416	2 • 6 1 2 9 6 5 • 0 3 6 3 2 1 0 • 9 1 3 7 8	3 • 3 26 46 6 • 267 0 3 6 • 5 66 37	4.00470 9.63353	^o el
0.50250			°1,2		
0.36855	0.33829		^σ 1,3	⁰ 2,3	,
0 - 2 3 5 8 2	0.22381	0.30344	etc.		
0.12211	0.12928	0.05921	0.26013		
0.05394	0.05507	0.05940	0 0+2702	0	
0.02149	0.02486	0.02912	0.00348	o	

Continued

0.00 866	0.01199	0.01122	0.00419	0	σ _{1,8}	°2.8	etc.
0 0.2146	7				1,90	∠ 90	
0.00463 0 0 0.2	0.00906 6991	0.00875	0.00308	0			
	- ,,						
၀•၀ ၀ ၀ ၀ ၀ ၀	0.00239 0.20583	0.00249	0.00107	0			
0.0000	0.00048	0.00050	0.000 *0	^			
0 0 0 0	0.00048	0.00033	0 * 0 0 0 1 9	V			
	0.00044	0.00050	0.00011	0			
0 0 0 0	0						
0.00001	0.00244	0.00205	ο _* ου ο 2 δ	٥			
0 0 0 0							
0 0.2891	I						
0 0.0009	9 0.0015	I 0.0004	3 0	•			
0 0 0 0	-						
0 0 0.0	2 2 9 7 ≠≠						

Table 4
Copper 14-group cross sections
averaged over FRO reflector spectrum

2 • 43 487 4 • 603 83 6 • 83579	2.60533 4.88695 7.55403	3.09346 5.33189 6.51493	3 6 1 3 6 3 6 6 • 46 9 6 6 6 • 8 4 7 6 2	4.28299 9.57789	^o tr
1.74028 0.26349 0.40021	0.81367 0.28186 0.25722	0.4787r 0.32583 0.17550	0.28660 0.25691 0.18505	0.27270 0.35963	^o ne
3 • 43270 4 • 83586 6 • 90396	3.15079 5.02779 7.63133	3.50097 5.39753 6.58209	4.03868 6.53548 6.91820	4.65766 9.67554	^σ T
1.09459 4.34035 6.43558	1.79166 4.60509 7.29682	2.61475 5.00606 6.33943	3•327 0 3 · 6•21275	4.01028 9.21826	^o el
0.51092			σ _{1,2}		
0.36980	0.33932		°1,₃3	°2,3	
0.23826	0.22439	0.27071	etc.		
0.12389	0.12991	0.06497	0.25196		
0.05487	0.05480	0.06144	0 0.257	4 3	
0.02189	0.02502	0.02969	a• 00 376	0	

0.00884 0.01217 0.01161 0.00446 0 01,8 02,8 etc.

0.00473 0.00932 0.00880 0.00321 0

0.00069 0.00248 0.00248 0.00111 0

0.00007 0.00050 0.00052 0.00020 0

0.00003 0.00046 0.00049 0.00011 0

0.00003 0.00046 0.00049 0.00011 0

0.00001 0.00258 0.00200 0.00029 0

0.00001 0.00258 0.00200 0.00029 0

0.00001 0.00258 0.00200 0.00029 0

0.00015 0.00146 0.00045 0

0 0 0 0 0

314 p#

Table 5
U-235 14-group cross sections
averaged over FRO core 1 spectrum

3.69910 3.52427 9.21900	3.39182 3.98238 11.63981		3 •00 723 3 • 53 299 43 • I 410		vo _f
4.30602 8.31483 16.48315	4.73031 9.81972 18.24211	11:28 78 1	5•3 5883 13•30165 3 36•821	14.58269	^σ tr
3.10010 2.18425 5.41032	2 • 9 573 I 2 • 43 566 6 • 9 49 63	2.56890 2.73076 II:75227	2 •0 79 99 3 •089 55 -2 5•099 41	2.05027 3.71836	σne
7•5 ² 577 9•8 59 ² 0 16•51465		6.589 13 18.149 70 23.30 619	7.11615 13.3306 3.62855	4 ~14.61359	$\sigma_{ extbf{T}}$
1 • 20 593 6 • 130 58 1 1 • 0 728 3	1 • 77300 7 • 38 40 5 	8 - 5570 5	3.27885 10.21210 5 11.722	10.86433	$\sigma_{ t el}$
0.46473			°1,2		
0 + 51 2 60	0 • 3 6630		σ _{1,3}	°2,3	
0 • 40 33 6	0 • 46490	0 • 60 3 43	etc.		
0 •2 388 2	0 • 3 4 4 5 6	0 • 3 7 59 6	0 + 51 537		
0.11485	0 -2 28 73	0 - 18371	0 • 20320	0.42676	
0 •0 48 19 0 •3 6000	0.11855	0 • 9 7 40 4	0 • 0 5 4 0 3	o•08968	

Continued

						Logi	0.0 0 0
			0	5 60000 O	6000000	8100000	0.00003
			00000°0	800000	60000*0	o† 000• 0	00000*0
						\$ 9	666 0 •0 0
			o	0 °00 II 5	Ikooo*o	9400000	7100000
			10000*0	\$1000*0	8500040	84 0000 0	7 000000
					٠		L9 860° 0
			•	À 8&000 G	021 000 0	\$6100°0	000000
			0100000	1 800000	08000.0	† 01 00° 0	80000=0
			0888000	eL\$00•0	\$ 92 90* 9	St 2000 0	1 8 0000 0
			0.00013	0.00033	4600000	0.00113	9100000
			,	₹ £ ₹60 * 0	765 10°0	9 87 1000	19 200*0
			19000*0	84100.0	944 0000	2880000	£9100°0
					9 66 o E • o	7 0 \$ 9 0 • 0	60280*0
			84110.0	88210.0	0.03133	0.01000	86010.0
						69115•0	0.00002
• ၁19	م2•8	$\mathfrak{F}^{\bullet}T_{\mathbf{p}}$	994 2000	0.02113	L\$ L 10° 0	18980.0	90020•0
- +-	-	_	7740-	V	50 1 10 7 7	- 0200	7

Table 6
U-235 14-group cross sections
averaged over FRO reflector spectrum

3•67369 3•5 2747 8•55939	3•38712 3•98954 11•89046	3.13681 4.51438 23.14617		νσ _f
4+34086 8-32882 16-19319	9.33983	11.27160	5.35003 6.67893 13.2674 14.89775 38.85723	o _{tr}
3.12157 2.19369 5.05859	2.95699 2.45988 6.96439	2 • 5 6 0 4 4 2 • 7 3 I 4 I I 4 • 4 2 4 0 5	2.07602 2.03881 3.03252 4.03299 27.15194	^o ne
7.53612 9.87115 16.22478	11.19559	12.14124	7.10721 8.34147 13.29651 14.92866 3 38.89053	$\sigma_{ extbf{T}}^{}$
6.13513		2.17782 8.54019 11.5412		^o el
0.46382		,	^σ 1,2	
0.51471	0.36085	i .	σ _{1,3} σ _{2,3}	
0.40861	0+45954	0.60450	etc.	
0.24317	0.34771	0.37093	0.50882	
0.11727	0.23404	0.16981	0.10417 0.41822	
0.04929 0.36639	0.12131	0.01423	0.05659 0.08914	

Continued

Table 6 (cont.)

0.02053 0.06362	0.03711	0. 21969	0.02136	0.02714	°1,8	°2,8	etc.
0.01124	0.01579	0.02476	0.01277	0.01112			
0.00167	0.00521	0.00512	0.00145	0.00078			
0.00017 0.00031	0.00112	0.00112 0.00166	0+00032 0+00359	0.00013			
0.00008 0.00029 0.01119	0.00103 0.00172	0.00096 0.00113	0.00030	0.00010			
0.00001 0.00014 0 0.0143	0.00048	0.00045	0.00014 0.00113	0.00001			
0 0 0 0 1 4 3 0 0 0 0 0 0 0 0 0 0 0 0 3	0.00039 0.00016	0.000011	0.00003 0.00025	0*00000			
•	5433 rt#			-			

Table 7
U-238 14-group cross sections
averaged over FRO core 1 spectrum

	1.08932 0 0	0 . 0 6 469	0.00337	0	νσ _f
	4-5965 4 10-18137 15-37109		13.007	13 13.78033	$\sigma_{ t r}$
2+95800 0+70263 0+81912	2•75 0 3 4 0•86391 0•81 441	1.41789 1.02971 0.72370	0.69912 0.56917 0.88606	0.67544 0.57979	^o ne
7-32287 9-69488 15-64139		6.63685 12.63292 13.0138		8.90760 07 13.81741 5 0 9	$\sigma_{ extbf{T}}$
1.22518 7.34708 14.78075	1.34620 9.31745 14.55668			6.24899 7 13.20054 741	^o el
0.60453			°1,2		
0.67512	0.69237		°1,3	°2,3	
0.53193	0.675.44	0.60698	etc.		
0-31537	0 • 4709 4	0.26593	0 • 5 42 49		
0.15185	0.25013	0.23423	0.00013	0 a 5 2 5 3 1	
0.06379 0.50308	0.11130	0.11257	0.00031	0.02227	

Continued

0.02657 0.02312	0.04795 0.59655	0.02776	0.00777	0	°1,8	σ _{2,8}	etc.
	0•02689 0•02749	0.008.09 0.71356	0.00653	o			
0.00216 0 0.0062		0.00151 34 0.1756		0			
0.0002I	•	0.00030 NOSI 0.0		9			
0.00011 0 0.0010 0.12942			0.00031	o .			
0.00002 0 0.0004 0 0.0458	.7 0 0.0		0.00014	o			
9,00000 0 0,000I	I 0 0.0		0.00003	o			

Table 8
U-238 l4-group cross sections
averaged over FRO reflector spectrum

-	0	0.07052 0.00346	
4.27518 8.06861 15.40795	4.58416 10.21583 15.49305	4.55945 5.67359 11.98912 12.9765 12.30534 12.455	g
2.98191 0.72020 0.08993	2.74974 0.89042 0.79191	10,3247 0.08441 1.04001 0.51328 0.75032 1.02748	0.655935 3.68339
7 • 32776 9 • 7 0 8 3 6 15 • 4 4 9 2 9	11.42201	6.63506 7.37060 13.62569 13.0136 13.33780 73.487	2 23.99 805
	9 - 3 2 5 4 3	3.13699 4.98698 10.94911 23.46532 11.55502 11.427	13.27747
0.60232			
0.67836	0.69231		
0.53914	0.67687	0.57413	
0.30122	0.47329	0.28848 0.52526	
0.15509	0.25181	0.24445 0.00011	0.51001
0.06524	0.11217	0.11530 0.00034	0.02157

Table 8 (cont.)

	•027 1 9 •02297	0.04835	0.02865	0.00839	0
		0.02713		0.00694	0
0	•00221 0•0062	0.00410 3 0.03276	0.00156	0.00149	0
		0.00041 4 0 0.01			0
0		0.00020 5 0 0.00		0.00032	٥
0		0.00003 1.0 0.00		0.00015	0
0		0.00000 0 0 0.00 5025		0.00004	0

Table 9

Composition of the core and reflector zones in volume percent.

Material	***************************************	Identification				
	Co	re	Refl	ector		
	1 and 2	3	R1	R2		
С	:	29.32				
CF ₂	0.206	0.206				
Cr	1.18	1.18	1.18	1.61		
Fe	4.84	4.84	4.84	6.04		
Ni	0.523	0.523	0.523	0.85		
Cu			- 88.0			
บ-235	17.59	11.70		0.43		
U - 238	70.13	4678		60.57		

Table 10 Lower energy boundary, \textbf{E}_{L^2} and fraction of fissions, χ_s in each group for different cross section sets.

Group	14 groups, set 2		ll group	ll groups, set l		s, set 1
no.	E _L MeV	χ	E _L MeV	х	E _L MeV	χ
1	2.25	0.338	2.25	0.338	1.35	0.574
2	1.35	0.236	1.35	0.236	0.5	0.294
3	0.825	0.178	0.825	0.178	0.18	0.099
14	0.5	0.116	0.5	0.116	0.067	0.025
5	0.3	0.066	0.3	0.066	0.0091	0.008
6	0.18	0.033	0.18	0.033	0.007	0
7 .	0.11	0.017	0.11	0.017		
8	0.067	0.008	0.067	0.008		
9	0.025	0.006	0.025	0.006		
10	0.0091	0.002	0.0091	0.002		
11	0.0055	0	0.001	0		
12	0.0021	0 .				
13	0,0005	0		3,3		
14	0.00012	0				

Table 11
Results of critical mass calculations for different assemblies.

Data	Number	Geometry		Core		Reflector		Error in %
set ·	of groups		Identi- fication	Radius cm	Mass kg U-235	Identi- fication	Thickness cm	of the exp. crit. mass
1	6	Cyl., H/D=1.0	1	15.24	73.8	R1	30	1.2
1	11	Spherical	2	17.25	71.3	R1.	30	1.7
1.	11	Spherical	5	17.33	72.3	RL	24	
1	11	Spherical	2	17.44	73.7	R1	20	
1	11	Spherical	2	17.82	78.7	R1	15	
1	11	Spherical	2	18.68	90.6	R1.	10	
1	11.	Spherical	2.	20.59	121.4	R1	. 5	
1	6	Spherical	5	17,15	70.1	RI	30	0.0
2	6	Cyl., H/D=0.996	1	15.07	71.0	R1	30	- 2.7
1	11	Spherical	2	19.69	106-1	R2	15	
1	11	Spherical	2	19.78	107.5	R2	13.9	
2	1h .	Spherical	5:	16.89	67.0	RI	30	- 4.4
2	6	Spherical	3	16.84	66.3	RI	30	- 5∘3
i.	11	Spherical	3	22.79	109.6	a 1	24	
2	1.34	Spherical	3	22,26	102.2	R1.	30	
J.	11	Spherical	EFR III/9A	25.74	157.9	A	30	1.6
3,	7	Sylogical.	ZPR III/12	28,89	279.0	A	30	4.1
3	21	Spirriosi.	ern iii/15	30.79	226,8	A	30	7.4
6 3 64	1.4	Inherical.	ma III/10	25.02	147.0	A	30	- 3.9

Table 12 Effective beta values for FR 0/2, obtained by DS₁ calculations. The superscript (28 or 25) refers to U-238 and U-235, respectively.

i	β(28) xl0 ⁴ i,eff	β ⁽²⁵⁾ ×10 ¹ βi,eff
1	0.46	1.55
2	4.48	9.76
3	5.29	8.61
l ₄	12.67	18.73
5	7.35	5.87
6	2.45	1.19

Table 13

Neutron generation time, Λ_{\bullet} for FRO/2, obtained by DS₄ calculations. τ and ρ are the corresponding persistent period and reactivity.

τs	ρ	л ж 10 ⁸
1 x 10 ⁻⁵	0.0054	5.43
5 x 10 ⁻⁷	0.0866	4.33

Table 14

Effective beta values for FRO/2, obtained by the use of diffusion theory and perturbation theory.

i	β ⁽²⁸⁾ x10 ¹ βi,eff	β ⁽²⁵⁾ ×10 ^μ βi,eff
1	0.357	1.86
2	3.54	9.99
3	4.19	8.86
4	10.15	19.44
5	5.82	6.03
6	1.95	1.23

Flux per unit lethergy in the centre of core 2.

Pig. 1

Full line: Cross section set 2, 14 groups.
Dotted line: Cross section set 1, 11 groups.

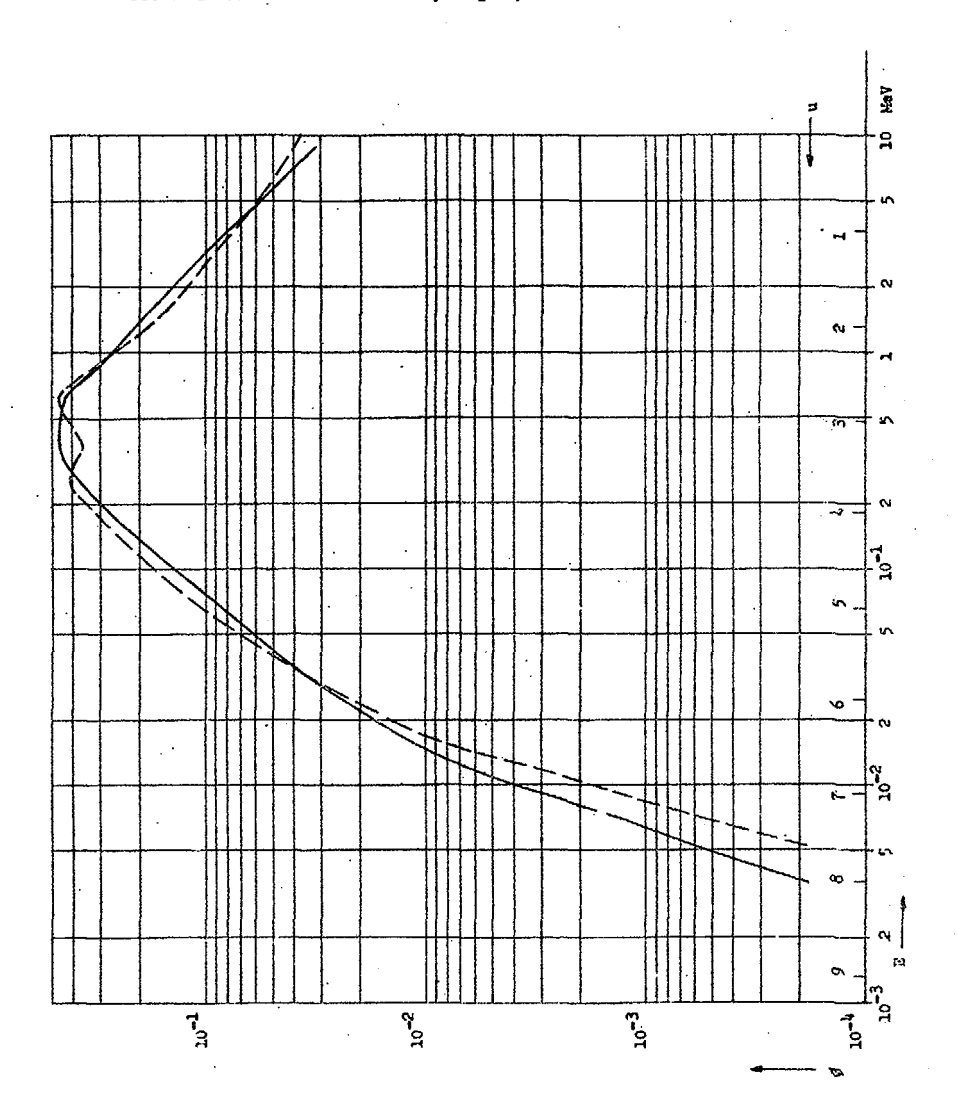
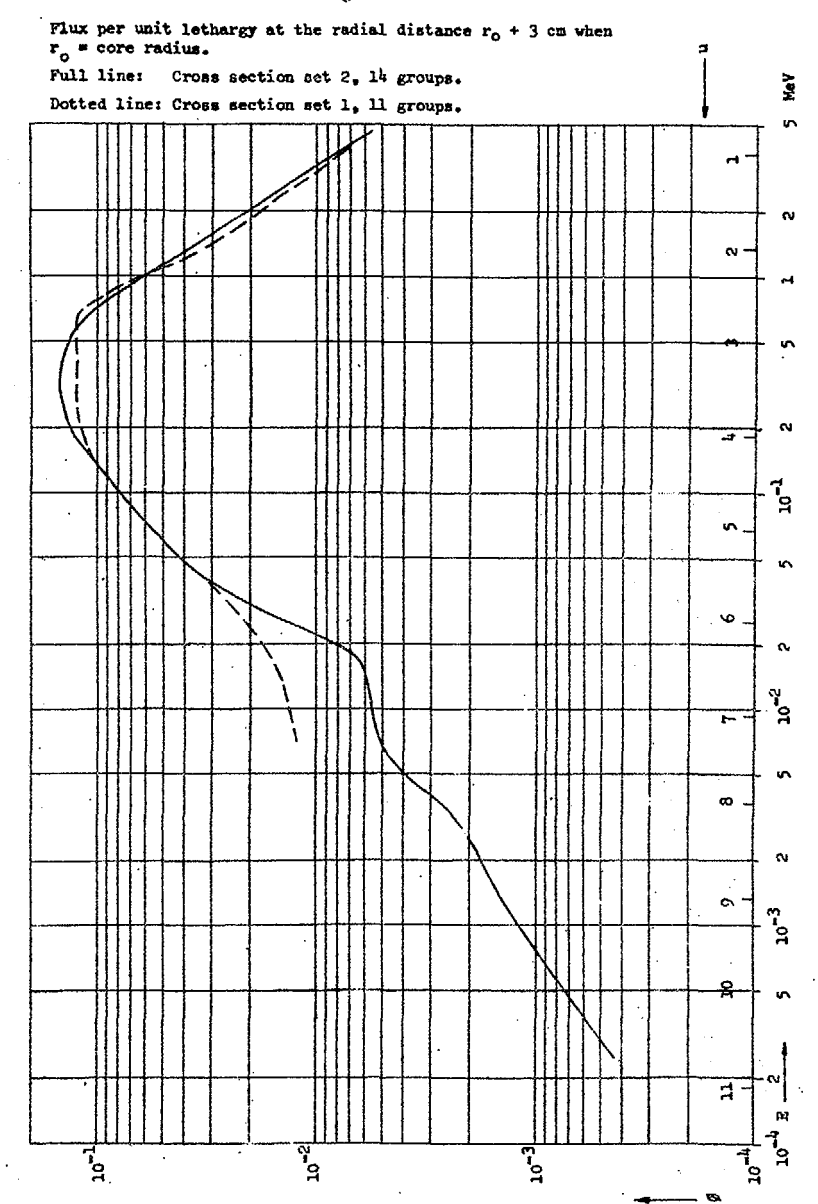


Fig. 2



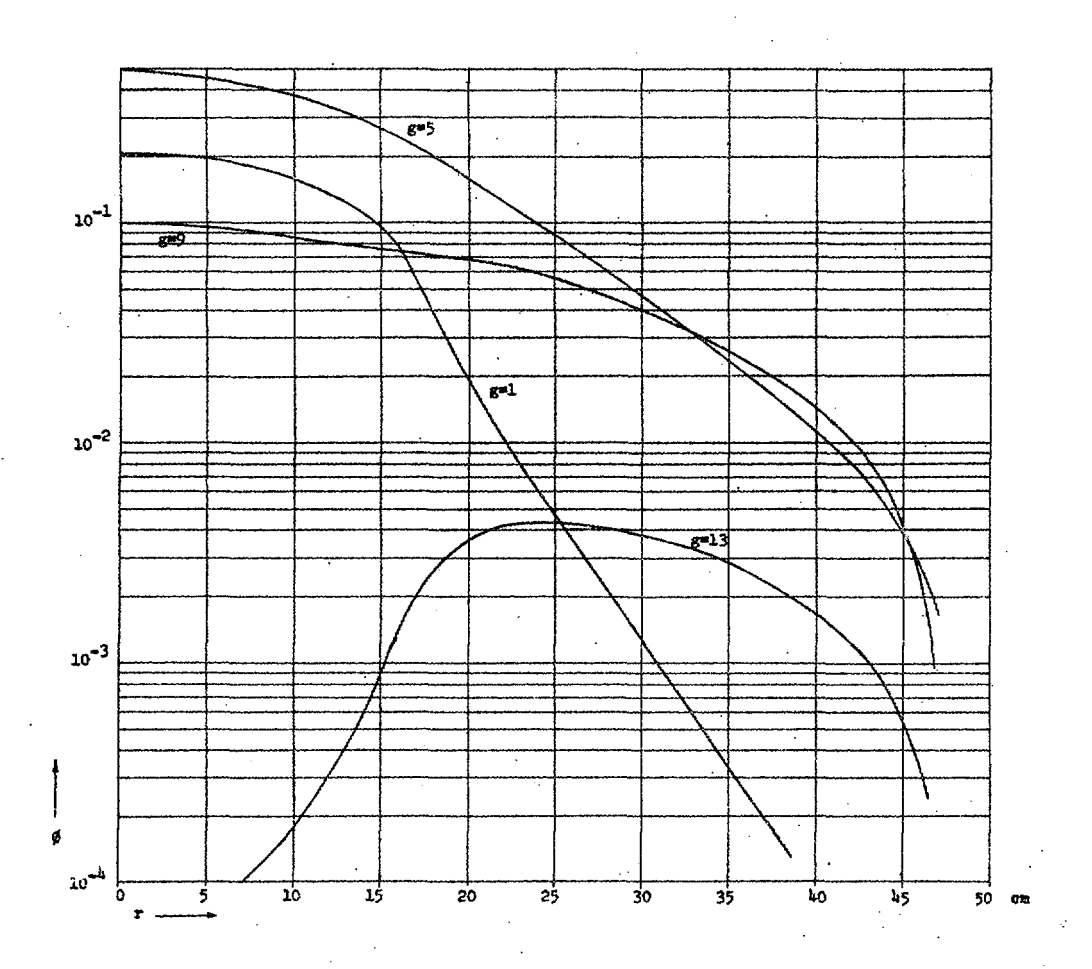


Fig. 3 Flux in the groups 1, 5, 9 and 13 as functions of radius. Assembly 2.

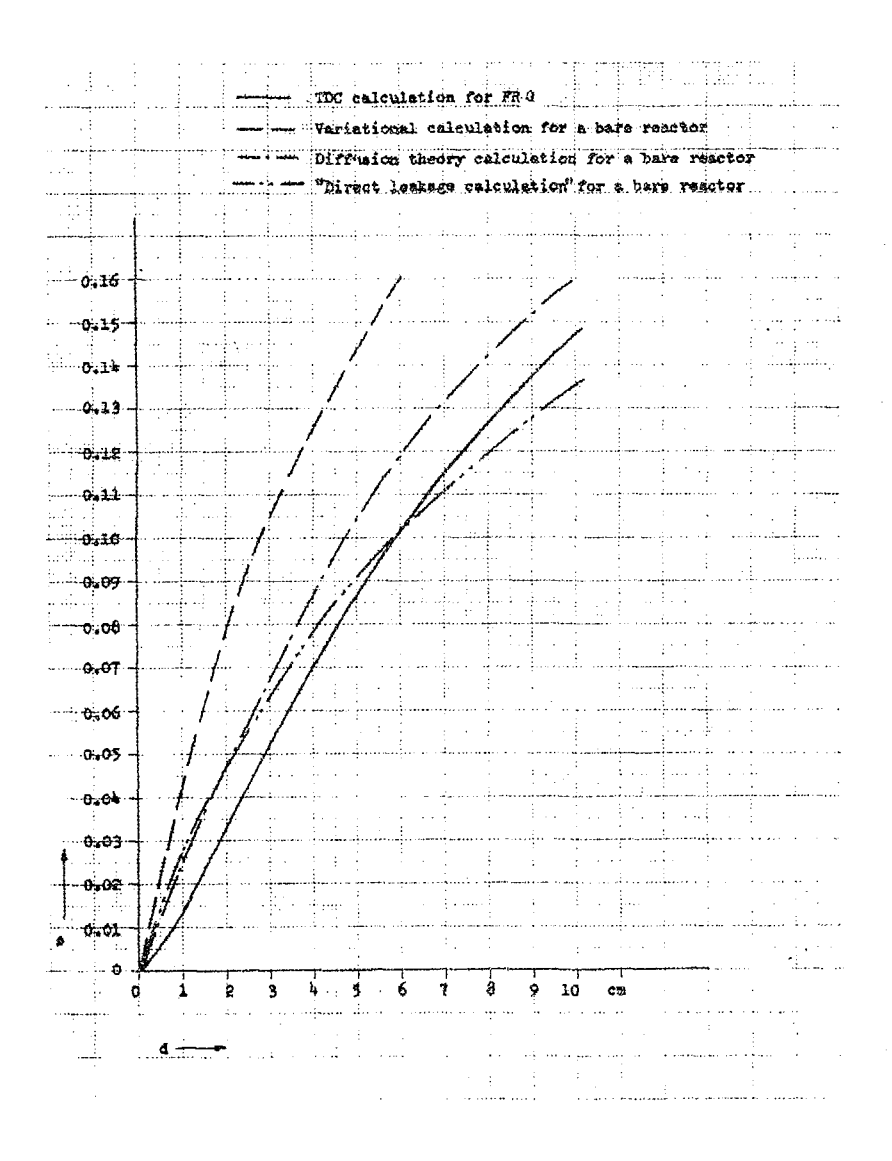


Fig. 4 Reactivity equivalence of the air gap, d.

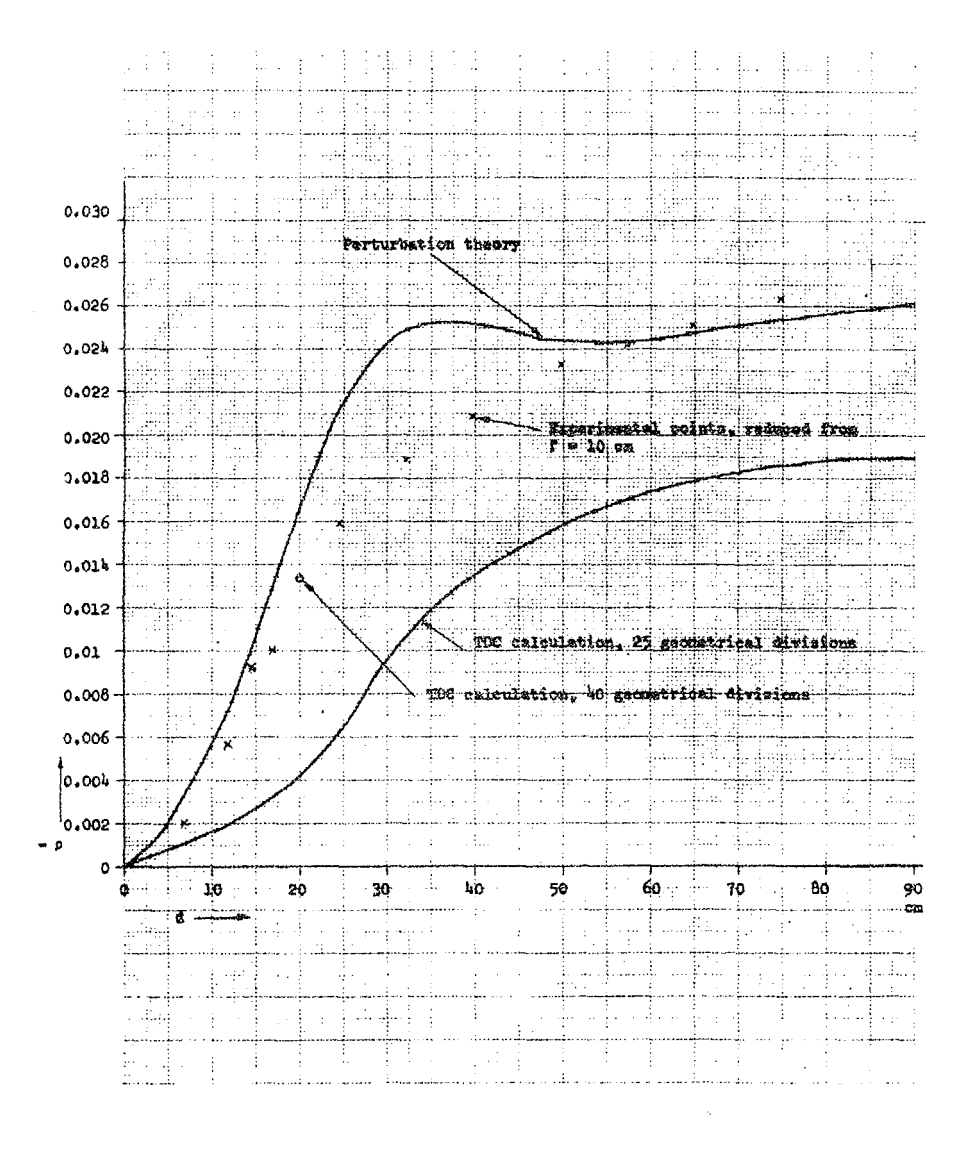


Fig. 5 Reactivity of FR 0/1 as a function of the position d of a central control rod.

LIST OF PUBLISHED AE-REPORTS

- 1—120. (See the back cover earlier reports.)
- 121. The transistor as low level switch. By A. Lydén. 1963. 47 p. Sw. cr. 8:--.
- 122. The planning of a small pilot plant for development work on aqueous reprocessing of nuclear fuels. By T. U. Sjöborg, E. Haeffner and Hultgren. 1963. 20 p. Sw. cr. 8:—.
- 123. The neutron spectrum in a uranium tube. By E. Johansson, E. Jonsson, M. Lindberg and J. Mednis. 1963. 36 p. Sw. cr. 8:—.
- 124. Simultaneous determination of 30 trace elements in cancerous and non-cancerous human tissue samples with gamma-ray spectrometry. K. Samsahl, D. Brune and P. O. Wester. 1963. 23 p. Sw. cr. 8:—.
 125. Measurement of the slowing-down and thermalization time of neutrons in water. By E. Möller and N. G. Sjöstrand. 1963. 42 p. Sw. cr. 8:—.
 126. Power as the processed by the state of the state
- 126. Report on the personell dosimetry at AB Atomenergi during 1962. By K.-A. Edvardsson and S. Hagsgård. 1963. 12 p. Sw. cr. 8:—.
- 127. A gas target with a tritium gas handling system. By B. Holmqvist and T. Wiedling, 1963. 12 p. Sw. cr. 8:—.
- 128. Optimization in activation analysis by means of epithermal neutrons.

 Determination of molybdenum in steel. By D. Brune and K. Jirlow. 1963.

 11 p. Sw. cr. 8:—. 11 p. Sw. cr. 8:-
- 129. The P₁-approximation for the distribution of neutrons from a pulsed source in hydrogen. By A. Claesson. 1963. 18 p. Sw. cr. 8:—.
- 130. Dislocation arrangements in deformed and neutron irrodiated zirconium and zircaloy-2. By R. B. Roy. 1963. 18 p. Sw. cr. 8:—.
- 131. Measurements of hydrodynamic instabilities, flow oscillations and burnout in a natural cirkulation loop. By K. M. Becker, R. P. Mathisen, O. Eklind and B. Norman. 1964. 21 p. Sw. cr. 8:—.
- 132. A neutron rem counter. By I. Ö. Andersson and J. Braun. 1964. 14 p. Sw. cr. 8:—.
- 133. Studies of water by scattering of slow neutrons. By K. Sköld, E. Pilcher and K. E. Larsson. 1964. 17 p. Sw. cr. 8:—.
 134. The amounts of As, Au, Br, Cu, Fe, Mo, Se, and Zn in normal and uraemic human whole blood. A comparison by means neutron activation analysis. By D. Brune, K. Samsahl and P. O. Wester. 1964. 10 p. Sw. cr. 8:—.
- 135. A Monte Carlo method för the analysis of gamma radiation transport from distributed sources in laminated shields. By M. Leimdörfer. 1964. 28 p. Sw. cr. 8:—.
- 136. Ejection of uranium atoms from UO₂ by fission fragments. By G. Nilsson. 1964. 38 p. Sw. cr. 8:—.
- 137. Personell neutron monitoring at AB Atomenergi. By S. Hagsgård and C.-O. Widell. 1964. 11 p. Sw. cr. 8:—.
- 138. Radiation induced precipitation in iron. By B. Solly. 1964. 8 p. Sw. cr.
- Angular distributions of neutrons from (p, n)-reactions in some mirror nuclei. By L. G. Strömberg, T. Wiedling and B. Holmqvist. 1964. 28 p. Sw. cr. 8:—.
- 140. An extended Greuling-Goertzel approximation with a P_n -approximation in the angular dependence. By R. Håkansson. 1964. 21 p. Sw. cr. 8:-
- 141. Heat transfer and pressure drop with rough surfaces, a literature survey. By A. Bhattachayya. 1964. 78 p. Sw. cr. 8:—.
- 142. Radiolysis of aqueous benzene solutions. By H. Christensen. 1964. 50 p.
- 143. Cross section measurements for some elements suited as thermal spect-rum indicators: Cd, Sm, Gd and Lu. By E. Sokolowski, H. Pekarek and E. Jonsson. 1964. 27 p. Sw. cr. 8:—.
- 144. A direction sensitive fast neutron monitor. By B. Antolkovic, B. Holmqvist and T. Wiedling. 1964. 14 p. Sw. cr. 8:—.
- 145. A user's manual for the NRN shield design method. By L. Hjärne. 1964. 107 p. Sw. cr. 10:—.
- 146. Concentration of 24 trace elements in human heart tissue determined by neutron activation analysis. By P. O. Wester. 1964. 33 p. Sw. cr. 8:—.
 147. Report on the personnel Dosimetry at AB Atomenergi during 1963. By K.-A. Edvardsson and S. Hagsgård. 1964. 16 p. Sw. cr. 8:—.
- 148. A calculation of the angular moments of the kernel for a monatomic gas scatterer. By R. Håkansson. 1964. 16 p. Sw. cr. 8:—.
- 149. An anion-exchange method for the separation of P-32 activity in neutron-irradited biological material. By K. Samsahl. 1964. 10 p. Sw. cr
- 150. Inelastic neutron scattering cross sections of Cu⁶ and Cu⁶⁵ in the energy region 0.7 to 1.4 MeV. By B. Holmqvist and T. Wiedling. 1964. 30 p. Sw. cr. 8:—.
- 15). Determination of magnesium in needle biopsy samples of muscle tissue by means of neutron activation analysis. By D. Brune and H. E. Sjöberg. 1964. 8 p. Sw. cr. 8:—.
- 152. Absolute El transition probabilities in the dofermed nuclei Yb¹⁷⁷ and Hf¹⁷⁹. By Sven G. Malmskog. 1964. 21 p. Sw. cr. 8:—.
- 153. Measurements of burnout conditions for flow of boiling water in vertical 3-rod and 7-rod clusters. By K. M. Becker, G. Hernborg and J. E. Flinta. 1964. 54 p. Sw. cr. 8:—.
- 154. Integral parameters of the thermal neutron scattering law. By S. N. Purohit. 1964. 48 p. Sw. cr. 8:—.
- 155. Tests of neutron spectrum calculations with the help of foil measurments in a D₂O and in an H₂O-moderated reactor and in reactor shields of concrete and iron. By R. Nilsson and E. Aalto. 1964. 23 p. Sw. cr. 8:—.
 156. Hydrodynamic instability and dynamic burnout in natural circulation two-phase flow. An experimental and thearetical study. By K. M. Becker. S. Jahnberg, I. Haga, P. T. Hansson and R. P. Mathisen. 1964. 41 p. Sw. cr. 8:—.
- 157. Measurements of neutron and gamma attenuation in massive laminated shields of concrete and a study of the accuracy of some methods of calculation. By E. Aalto and R. Nilsson. 1964. 110 p. Sw. cr. 10:—.
- 158. A study of the angular distributions of neutrons from the Be⁹ (p,n) B⁹ reaction at low proton energies. By. B. Antolkovic', B. Holmqvist and T. Wiedling. 1964. 19 p. Sw. cr. 8:—.
- 159. A simple apparatus for fast ion exchange separations. By K. Samsahl. 1964. 15 p. Sw. cr. 8:—.
 160. Measurements of the Fe⁵⁴ (n, p) Mn⁵⁴ reaction cross section in the neutron energy range 2.3—3.8 MeV. By A. Lauber and S. Malmskog. 1964. 13 p. Sw. cr. 8:—.

- 161. Comparisons of measured and calculated neutron fluxes in laminated iron and heavy water. By. E. Aalto. 1964. 15 p. Sw. cr. 8:—.
- 162. A needle-type p-i-n junction semiconductor detector for in-vivo measurement of beta tracer activity. By A. Lauber and B. Rosencrantz. 1964. 12 p. Sw. cr. 8:—.
- 163. Flame spectro photometric determination of strontium in water and biological material. By G. Jönsson. 1964. 12 p. Sw. cr. 8:—.
- 164. The solution of a velocity-dependent slowing-down problem using case's eigenfunction expansion. By A. Claesson. 1964. 16 p. Sw. cr. 8:—.
- 165. Measurements of the effects of spacers on the burnout conditions for flow of boiling water in a vertical annulus and a vertical 7-rod cluster. By K. M. Becker and G. Hernberg. 1964. 15 p. Sw. cr. 8:—.
- 166. The transmission of thermal and fast neutrons in air filled annular ducts through slabs of iron and heavy water. By J. Nilsson and R. Sandlin. 1964. 33 p. Sw. cr. 8:—.
- 167. The radio-thermoluminescense of CaSO₄: Sm and its use in dosimetry. By B. Bjärngard. 1964. 31 p. Sw. cr. 8:—.
 168. A fast radiochemical method for the determination of some essential trace elements in biology and medicine. By K. Samsahl. 1964. 12 p. Sw. cr. 8:—
- 169. Concentration of 17 elements in subcellular fractions of beef heart tissue determined by neutron activation analysis. By P. O. Wester. 1964. 29 p. Sw. r. 8.—
- 173. Formation of nitrogen-13, fluorine-17, and fluorine-18 in reactor-irradiated H₂O and D₂O and applications to activation analysis and fast neutron flux monitoring. By L. Hammar and S. Forsén. 1964. 25 p. Sw. cr. 8:—.
- 171. Measurements on background and fall-out radioactivity in samples from the Baltic bay of Tvären, 1957—1963. By P. O. Agnedal. 1965. 48 p. Sw. cr. 8:—
- 172. Recoil reactions in neutron-activation analysis. By D. Brune. 1965. 24 p. Sw. cr. 8:—-.
- 173. A parametric study of a constant-Mach-number MHD generator with nuclear ionization. By J. Braun. 1965. 23 p. Sw. cr. 8:—.
 174. Improvements in applied gamma-ray spectrometry with germanium semi-conductor dector. By D. Brune, J. Dubois and S. Hellström. 1965. 17 p. Sw. cr. 8:—.
- 175. Analysis of linear MHD power generators. By E. A. Witalis. 1965. 37 p. Sw. cr. 8:—.
- 176. Effect of buoyancy on forced convection heat tranfer in vertical channels a literature survey. By A. Bhattacharyya. 1965. 27 p. Sw. cr. 8:—.
 177. Burnout data for flow of boiling water in vertical round ducts, annuli and rod clusters. By K. M. Becker, G. Hernborg, M. Bode and O. Erikson. 1965. 109 p. Sw. cr. 8:—.
- 178. An analytical and experimental study of burnout conditions in vertical round ducts. By K. M. Becker. 1965. 161 p. Sw. cr. 8:—.
 179. Hindered El transitions in Eu¹⁵⁵ and Tb¹⁶¹. By S. G. Malmskog. 1965. 19 p.
- Photomultiplier tubes for low level Cerenkov detectors. By O. Strinde-hag. 1965. 25 p. Sw. cr. 8:—.
- 181. Studies of the fission integrals of U235 and Pu239 with cadmium and boron filters. By E. Hellstrand. 1965. 32 p. Sw. cr. 8:—.
- 182. The handling of liquid waste at the research station of Studsvik, Sweden. By S. Lindhe and P. Linder. 1965. 18 p. Sw. cr. 8:—.
 183. Mechanical and instrumental experiences from the erection, commissioning and operation of a small pilot plant for development work on aqueous reprocessing of nuclear fuels. By K. Jönsson. 1965. 21 p. Sw. cr. 8:—
- 184. Energy dependent removal cross-sections in fast neutron shielding theory. By H. Grönroos. 1965. 75 p. Sw. cr. 8:—.
 185. A new method for predicting the penetration and slowing-down of neutrons in reactor shields. By L. Hjärne and M. Leimdörfer. 1965. 21 p. Sw. cr. 8:—.
- 186. An electron microscope study of the thermal neutron induced lass in high temperature tensile ductility of Nb stabilized austenitic steels. By R. B. Roy. 1965. 15 p. Sw. cr. 8:—.
- 187. The non-destructive determination of burn-up means of the Pr-144 2.18 MeV gamma activity. By R. S. Forsyth and W. H. Blackadder. 1965. 22 p. Sw. cr. 8:—.
- 188. Trace elements in human myocardial infarction determined by neutron activation analysis. By P. O. Wester. 1965. 34 p. Sw. cr. 8:—.
 189. An electromagnet far precession of the polarization of fast-neutrons. By O. Aspelund, J. Bäckman and G. Trumpy. 1965. 28 p. Sw. cr. 8:—.
- 190. On the use of importance sampling in particle transport problems. By B. Eriksson. 1965. 27 p. Sw. cr. 8:---.
- 191. Trace elements in the conductive tissue of beef heart determined by neutron activation analysis. By P. O. Wester. 1965. 19 p. Sw. cr. 8:—.
 192. Radiolysis of aqueous benzene solutions in the presence of inorganic oxides. By H. Christensen. 12 p. 1965. Sw. cr. 8:—.
- 193. Radiolysis of aqueous benzene solutions at higher temperatures. By H. Christensen. 1965. 14 p. Sw. cr. 8:—.
- 194. Theoretical work for the fast zero-power reactor FR-0. By H. Häggblom. 1965. 45 p. Sw. cr. 8:—.

Förteckning över publicerade AES-rapporter

- 1. Analys medelst gamma-spektrometri. Av D. Brune. 1961. 10 s. Kr 6:—.
- Bestrålningsförändringar och neutronatmosfär i reaktortrycktankar -några synpunkter. Av M. Grounes. 1962. 33 s. Kr 6:--.
- 3. Studium av sträckgränsen i mjukt stål. Av G. Östberg och R. Attermo. 1963. 17 s. Kr 6:—.
- Teknisk upphandling inom reaktorområdet. Av Erik Jonson. 1963. 64 s. Kr 8:—.
- Agesta Kraftvärmeverk. Sammanställning av tekniska data, beskrivningar m. m. fär reaktordelen. Av B. Lilliehöök. 1964. 336 s. Kr 15:—.

Additional copies available at the library of AB Atomenergi, Studsvık, Nyköping, Sweden. Iransparent microcards of the reports are obtainable through the International Documentation Center, Tumba, Sweden.